LONG-TERM NITRATE EXPORT PATTERN FROM HUBBARD BROOK WATERSHED 6 DRIVEN BY CLIMATIC VARIATION

BONGGHI HONG[1,*], DENNIS P. SWANEY[1], PETER B. WOODBURY[1,2] and DAVID A. WEINSTEIN[1]

[1]*Boyce Thompson Institute for Plant Research, Cornell University, Tower Road, Ithaca, NY 14853;*
[2]*USDA Forest Service, Northeastern Research Station, P.O. Box 640, Durham, NH 03824*
*(*author for correspondence, current address: 106 Illick Hall, SUNY-ESF, 1 Forestry Drive, Syracuse, NY 13210, e-mail: bh43@cornell.edu, Tel: 315-470-6768, Fax: 315-470-6934)*

(Received 18 November 2003; accepted 2 September 2004)

Abstract. From 1964 through 1994, the pattern of nitrate (NO_3^-) export from Watershed 6 at Hubbard Brook Experimental Forest (HBEF) in New Hampshire, U.S.A., exhibited 10 years of high export (1968–1977) followed by 12 years of low export (1978–1989), with four 'spikes' in 1970, 1973, 1976, and 1990. Disruptions of N cycling by soil freezing, insect defoliation, or drought have been suggested to explain this pattern. We developed a model of nitrogen dynamics demonstrating that most of the long-term pattern can be reproduced without explicit consideration of these events. Comparisons of simulated N fluxes between high and low export years suggested that inorganic N input to the soil, from both atmospheric N deposition and N mineralization, was significantly higher during periods of high streamflow NO_3^- flux than in low periods. Simulated inorganic N pools (ammonium and nitrate) and fluxes (nitrification, plant uptake, denitrification, and ammonia volatilization) were also significantly higher in these periods. By swapping the time sequences of inorganic N input between high and low export years, it was shown that N mineralization, not atmospheric N deposition, drives the simulated long-term pattern. Although simulated nitrification showed a stronger relationship with measured streamflow NO_3^- flux than did N mineralization, nitrification rate depended upon availability of soil ammonium supplied from N mineralization. Because N mineralization in the model varies only with soil temperature and moisture, we conclude that shifts in the interaction of these two variables over time produced the shifts in NO_3^- stream exports.

Keywords: biogeochemistry, forested watershed, Hubbard Brook, modeling, nitrogen dynamics, streamflow nitrate flux

1. Introduction

Nitrate (NO_3^-) exports from forested watersheds in the northeastern United States have changed dramatically over the past decades (Likens and Bormann, 1995), despite relatively little change in NO_x emissions and nitrogen deposition (Driscoll *et al.*, 2001; Aber *et al.*, 1998). The magnitude of this streamwater NO_3^- flux is small relative to other N fluxes such as N mineralization and plant uptake (Bormann *et al.*, 1977), but it is of great concern because of its potential environmental impacts, e.g. depletion of cations from soil (Likens *et al.*, 1998), increased aluminum transport (Henriksen *et al.*, 1988), eutrophication (Hecky and Kilham, 1988), and decreased stream and lake water quality (Murdoch and

Water, Air, and Soil Pollution **160:** 293–326, 2005.

Stoddard, 1992). Studies at the Hubbard Brook Experimental Forest (HBEF) have documented several of these changes during recent decades (e.g. Likens *et al.*, 1998).

Long-term catchment monitoring of HBEF has produced one of the most site-intensive data sets in the world, including more than three decades of streamflow NO_3^- flux data available on the World Wide Web (http://www.hubbardbrook.org/). At HBEF watershed 6 (W6), a biogeochemical reference watershed not subject to any experimental treatment, the long-term pattern of NO_3^- export from W6 during 1964 to 1994 (calendar year) can be characterized as exhibiting 10 successive years of relatively high NO_3^- export (1968–1977; mean = 0.46 g-N m^{-2} per year) including three spikes in 1970, 1973, and 1976, followed by 12 years of low NO_3^- export (1978–1989; mean = 0.14 g-N m^{-2} per year) and a subsequent spike in 1990. Several hypotheses focusing on disruption of N cycling by events such as soil freezing, insect defoliation, and drought have been suggested to explain the NO_3^- export pattern observed at HBEF W6. Likens and Bormann (1995) suggested that soil-freezing events during the winters of 1969–1970 and 1973–1974 preceded high stream NO_3^- concentrations in subsequent years. Mitchell *et al.* (1996) suggested that the extremely cold and dry period in the winter of 1989–1990 could have been responsible for the synchronous peaks in streamflow NO_3^- flux observed in 1990 at four forested watersheds of the northeastern United States including HBEF W6. A snow removal experiment at HBEF induced soil freezing and increased fine root mortality, soil NO_3^- concentrations, and NO_3^- leaching (Groffman *et al.*, 2001; Tierney *et al.*, 2001; Fitzhugh *et al.*, 2001, 2003). The outbreak of a defoliating caterpillar during 1969–1971 period was suspected to be an important reason for the high NO_3^- export from HBEF W6 during the 1970s (Eshleman *et al.*, 1998), although this view has been questioned (Lovett *et al.*, 1998, 2002). Murdoch *et al.* (2000) observed that an extended period of drought is frequently followed by many years of high stream NO_3^- export. Aber and Driscoll (1997) suggested that long-term, decadal timescale responses to severe drought in early 1960s might be responsible for high stream N at HBEF W6 in the 1970s and that elevated losses of N in the 1970s, which reduced the N availability in the soil, could be the reason for the low stream N in the 1980s.

Recently, Aber *et al.* (2002) have suggested that the pattern of NO_3^- export from Hubbard Brook can be explained only by invoking multiple climate and disturbance mechanisms. However, the possibility that the observed stream NO_3^- export pattern is related to simple interannual variations in climatic conditions has not been sufficiently explored. Soil microbial processes responsible for producing and exporting inorganic N are regulated by temperature and moisture in the soil (Christ *et al.*, 2002), so variations in these environmental conditions could produce changes in soil processes. Mean annual air temperature was shown to be correlated with stream NO_3^- concentrations at the Biscuit Brook watershed in the Catskill Mountains, NY (Murdoch *et al.*, 1998). Irrigation experiments induced increases in net N mineralization rates and NO_3^- leaching at European

EXMAN (experimental manipulation of forest ecosystems) sites (Tietema *et al.*, 1997).

The aim of this study was to investigate how much of the interannual variation in the stream NO_3^- at HBEF W6 can be explained simply by daily variation in environmental factors such as precipitation and temperature. We used SINIC (Simple Nitrogen Cycle model), a hydrologically driven model with relatively simple nitrogen dynamics that uses a daily time step. Because the model does not explicitly consider processes of soil freezing, insect defoliation, and long term effects of drought, we were able to evaluate the joint effects of daily temperature and moisture variation on decadal NO_3^- export patterns in the absence of these processes.

2. Model Description, Parameterization, and Evaluation Methodology

SINIC resulted from our effort to develop a simple model of N cycling for a range of forested watersheds, using available literature descriptions of major N flux processes. Because we sought to develop a model that would be applicable to a wide variety of sites, some processes (e.g. ammonia volatilization) were included that may not be important in HBEF W6. Our goal was to predict monthly streamflow and NO_3^- flux, which necessitated simulation at a finer time resolution. Daily meteorological data used to drive the model were obtained from the Hubbard Brook LTER website (http://www.hbrook.sr.unh.edu/data/data.htm).

SINIC was constructed within ECLPSS, a generic ecological modeling platform for spatially-explicit models (Woodbury *et al.*, 2002). It is currently programmed in MATLAB (http://www.mathworks.com/). Although we have experimented with spatially disaggregated versions of the model (i.e. at various 'cell' sizes from 10 m to 363 m spanning the HBEF W6), we found a single-cell, two-layer, spatially aggregated version characterizes the hydrological and nitrogen dynamics of HBEF W6 sufficiently well to reproduce much of the long-term variation of streamflow and NO_3^- losses.

Hydrologic processes considered in SINIC include daily precipitation/snowpack generation/snowmelt, evapotranspiration, vertical water fluxes between soil layers, infiltration-excess and saturation-excess runoff, and groundwater flow (Figure 1A). Nitrogen processes include atmospheric input of NH_4^+ and NO_3^- (wet/dry/snowmelt), mineralization of organic N, plant uptake of NH_4^+ and NO_3^-, nitrification, denitrification, ammonia volatilization, and vertical fluxes of NO_3^- between soil layers/discharge into stream channels (Figure 1B). A full mathematical description of each of these processes is available in Hong (2004) and also on the internet (http://cycas.cornell.edu/ebp/ebpspec/hong_phd/hong_thesis.html). Below, we describe the most important processes briefly, emphasizing novel aspects of the characterization of nitrogen processes.

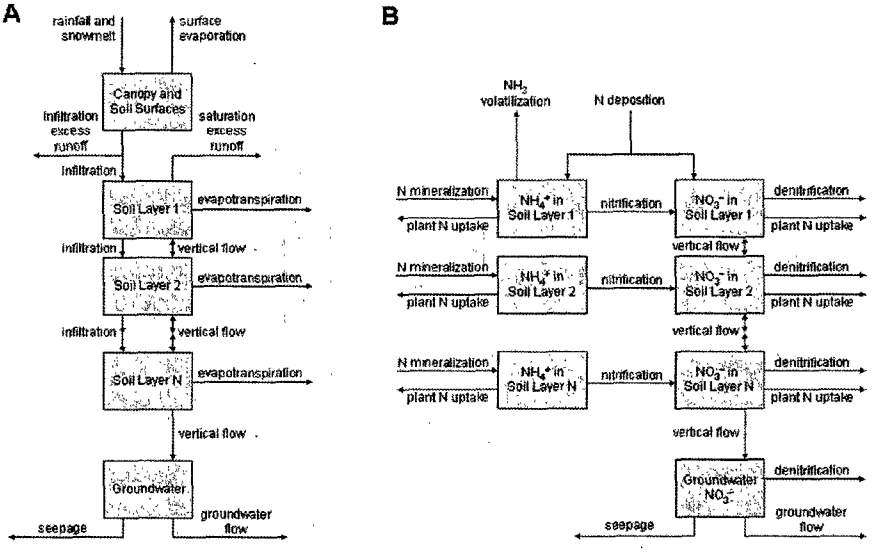

Figure 1. Structure of hydrologic components in SINIC, including soil water pools and fluxes (A), and structure of nitrogen components in SINIC, including nitrogen pools and fluxes (B).

2.1. HYDROLOGIC PROCESSES

2.1.1. *Daily Precipitation/Snowpack Generation/Snowmelt*

Precipitation is assumed to fall as snow when air temperature is below 0 °C. Snowmelt is assumed to occur at a rate proportional to the temperature above freezing (Gray and Prowse, 1993), and the proportion of the time in which this occurs is determined by a sinusoidal interpolation between daily max and min temperature.

2.1.2. *Evapotranspiration*

Daily potential evapotranspiration (PET) is calculated using the Penman-Monteith equation (Shuttleworth, 1993) adjusted for leaf area index (LAI) using the approach of Federer (1995). PET is partitioned to the various soil layers in proportion to the presence of roots, and estimation of soil moisture-limited evapotranspiration (ET) follows the Thornthwaite-Mather procedure (Steenhuis and Van Der Molen, 1986). Surface water is lost by evaporation (Rutter *et al.*, 1971).

2.1.3. *Vertical Water Flux*

Vertical flows redistribute soil water among soil layers. Downward movement of soil water in all soil layers except the bottom layer is based on Darcy's law, assuming gravity flow under unsaturated conditions (Bouraoui *et al.*, 1997). Under saturated conditions, water draining from the bottom soil layer is added to the groundwater pool.

2.1.4. *Runoff*

Runoff can be generated from either 'infiltration excess' or 'saturation excess' mechanisms. Infiltration excess runoff is governed by the Soil Conservation Service runoff equation (Rawls *et al.*, 1993). Infiltrated water is assumed to be distributed into all soil layers due to the presence of macropores (Federer, 1995). Saturation excess runoff occurs when soil moisture exceeds the saturated value of the entire soil (Zollweg, 1994).

2.1.5. *Groundwater/Baseflow*

Groundwater is considered a first-order reservoir in which the baseflow component of daily streamflow is proportional to the residual water in the groundwater pool. Seepage losses to deep aquifers at Hubbard Brook are assumed negligible (Federer, 1995).

2.2. Nitrogen Pools and Driving Processes

N mineralization, nitrification, and plant N uptake are very important components of N dynamics in the forested ecosystem, and the relative sizes of these fluxes may determine the amount and seasonality of nitrogen export (Johnson, 1992; Rosswall, 1982; Schmidt, 1982). Two species of nitrogen are considered in SINIC: ammonium (NH_4^+) and nitrate (NO_3^-). Because the total pool of organic nitrogen in soil is large compared to the inorganic pools (Bormann *et al.*, 1977) and much of it is recalcitrant to microbial action on annual or even longer time scales (Parton *et al.*, 1993), we consider N mineralization as an exogenous input of N to the NH_4^+ pool, governed by microbial activity, in which variations are driven only by soil temperature and moisture. Daily soil moisture within each layer is obtained from simulation of the soil water mass balance. Soil temperature is modeled as a damped, lagged response to daily average atmospheric temperature (Campbell and Norman, 1998). Soil temperature at 15 cm depth at HBEF, measured at approximately weekly intervals, was well predicted by this approach (observed mean = 8.68 °C, $n = 1050$, from http://www.hbrook.sr.unh.edu/data/soil/soil.htm; predicted mean = 8.31 °C; $r^2 = 0.88$).

2.2.1. *Wet and Dry Deposition/Snowmelt Input*

Daily wet deposition is estimated from monthly volume-weighted concentrations of NH_4^+ and NO_3^- in precipitation obtained from bulk precipitation collectors and daily measurements of precipitation (http://www.hubbardbrook.org/research/data/atmos/atmos.htm). Dry deposition data include weekly average nitrogen flux rates aggregated from hourly measurements of concentration and estimates of deposition velocity (http://www.epa.gov/castnet/data.html). Values of HNO_3 deposition and particulate NO_3^- deposition are combined as a 'total' NO_3^- dry deposition. Weekly average values of dry deposition of NH_4^+ and NO_3^- are divided by seven to obtain daily estimates. The record has gaps for several months;

values for missing months are replaced with monthly values averaged over the entire period of record. When precipitation occurs as a snowfall, it is assumed that the calculated daily total (wet + dry) N deposition is added to the snowpack. During snowmelt events, the amount of N released from the snowpack is calculated as snowmelt volume multiplied by the snowpack N concentration. This adjusted daily total N deposition is added to the top soil layer each day of the simulation.

2.2.2. *Mineralization of Organic N*

As stated earlier, mineralization of organic N is considered to vary with soil temperature and moisture only. The temperature relationship is based on a Q_{10} factor of Johnsson *et al.* (1987) modified in two respects: (1) following the Century model (Parton *et al.*, 1983), the temperature factor is set to zero at temperatures below 0 °C, and (2) the Q_{10} term is multiplied by a modifying term (T_{soil}/T_b) to ensure a smooth transition between 0 °C and the Q_{10} base temperature, T_b. The resulting temperature factor is:

$$f_T = \begin{cases} 0, & T_{soil} \leq 0 \\ Q_{10}^{(T_{soil}-T_b/10)} \times \frac{T_{soil}}{T_b}, & 0 < T_{soil} \leq T_b \\ Q_{10}^{(T_{soil}-T_b/10)}, & T_b < T_{soil} \end{cases} \quad (1)$$

where f_T is the Q_{10} soil temperature factor; T_{soil} the daily mean soil temperature (°C); Q_{10} the factor change in rate with a 10 °C change in temperature; T_b the base temperature at which Q_{10} factor equals 1 (°C).

A soil moisture factor is calculated using the moisture content in the soil, which is available from the hydrologic component of the model. If the soil moisture is below the saturation and above the wilting point, there is no restriction in N mineralization by soil moisture, and N mineralization proceeds at a rate determined by soil temperature. At or above saturation, the mineralization rate becomes zero because the soil becomes anaerobic (Johnsson *et al.*, 1987). N mineralization is also zero at or below wilting point:

$$f_M = \begin{cases} 1, & \theta_w < \theta < \theta_{sat} \\ 0, & \text{otherwise} \end{cases} \quad (2)$$

where f_M is the soil moisture factor; θ_w the soil water content at wilting point (m^3 water m^{-3} soil); θ the soil water content (m^3 water m^{-3} soil); θ_{sat} the soil water content at saturation (m^3 water m^{-3} soil).

The daily net N mineralization rate under 'optimal' conditions, assumed to be a fixed value, can in principle, be obtained from experimental soil incubation studies (Schmidt, 1982). We estimate daily values of mineralization under conditions of suboptimal soil temperature and moisture mediated by the temperature and moisture

factors as:

$$F_{min} = k_{min} \times f_T \times f_M \tag{3}$$

where F_{min} is the daily net N mineralization rate (g-N m^{-2} per day); k_{min} the daily net N mineralization rate under 'optimal' conditions (g-N m^{-2} per day).

Thus soil temperature controls mineralization on days in which soil moisture falls within an optimal range and soil moisture eliminates mineralization on days that are too wet or too dry. While we could add more detail related to soil moisture controls on N mineralization, we found the joint effect of temperature and moisture as parameterized adequate and simple.

2.2.3. *Plant N Uptake*

Nitrogen uptake is calculated as the smaller of two values, the potential plant N demand and the available N in the soil. The potential plant N demand over time is represented by a simple trapezoid-shaped function defined by an initial day of uptake each year, the first day when maximum uptake is possible, the last day when maximum uptake is possible, and a final day of uptake. A scaling factor is applied to calculate daily plant N demand from annual N demand, and distributed among soil layers according to the proportion of nitrogen-absorbing roots in each soil layer:

$$D_{day}(i, t) = \frac{R(t)}{A_R} \times D_{year} \times f_{root}(i) \tag{4}$$

where $D_{day}(i,t)$ is the daily plant N demand in the ith soil layer on day t (g-N m^{-2} per day); $R(t)$ the relative daily plant N demand on day t; A_R the integral of $R(t)$ over the entire year; D_{year} = annual plant N demand (g-N m^{-2} per year); $f_{root}(i)$ the fraction of roots in the ith soil layer.

Equation (4) scales relative plant N demand, so that the integrated daily plant N demand over the year equals annual plant N demand (D_{year}). The D_{year} represents the maximum amount of N that can be taken up by the plants when soil N availability does not restrict plant N uptake throughout the year, but actual plant N uptake is likely to be lower than plant N demand because of the limitation of soil N availability. Equal affinity for NH_4^+ and NO_3^- is assumed as in PnET-BGC (Gbondo-Tugbawa *et al.*, 2001), so demand is divided into corresponding NH_4^+ and NO_3^- demands according to their relative concentrations. The calculation of plant N uptake is made from bottom to top soil layers. Any unsatisfied daily plant N demand due to insufficient soil N in lower soil layers is added to the N demand in the upper soil layer. However, unsatisfied plant N demand is not accumulated over time.

2.2.4. *Nitrification*

Nitrification is simulated as a first-order decay process of soil NH_4^+, with the 'optimum' rate modified by the temperature and moisture factors identical to those

for N mineralization:

$$F_{\text{nit}} = k_{\text{nit}} \times N_{\text{NH4}} \times f_{\text{T}} \times f_{\text{M}} \tag{5}$$

where F_{nit} is the daily net nitrification rate (g-N m^{-2} per day); k_{nit} the decay constant for nitrification (per day); N_{NH4} the soil ammonium concentration (g-N m^{-2}).

2.2.5. *Denitrification and Ammonia Volatilization*
The equation describing denitrification follows Johnsson *et al.* (1987) without modification. The rate of ammonia volatilization is calculated assuming that (1) ammonia (in gaseous form) is in equilibrium with ammonium (in aqueous form) (Loehr *et al.*, 1973), (2) the ammonia is uniformly distributed through the soil layer, and (3) all of the ammonia in top centimeter of soil is lost each day.

2.2.6. *Vertical Flow, Groundwater Flow, and Seepage*
Nitrate is assumed to be the only mobile form of inorganic nitrogen, as the ammonium cation is assumed held by negatively charged soil and organic matter colloids. Downward vertical flow of water carries NO_3^- in soil to the groundwater NO_3^- pool, and NO_3^- in groundwater is discharged to the stream. Nitrate fluxes corresponding to each of the water fluxes are calculated as the product of the water flow rate and the NO_3^- concentration in the pool from which the water flow originates.

2.3. Parameterization

Table I (hydrologic processes) and II (nitrogen processes) list all the parameters in SINIC used to simulate the NO_3^- export from HBEF W6 during the period of 1964–1994. A detailed description of the full parameterization process is available on the internet (http://cycas.cornell.edu/ebp/ebpspec/hong_phd/hong_thesis.html). Here we highlight the most important parameters.

Although SINIC can have multiple soil layers with distributed root densities, for simplicity it is assumed that: (1) the total soil depth at HBEF W6 is 70 cm (Federer, 1995), and (2) many important biological activities, such as N mineralization and uptake of water and nitrogen by plant roots, are concentrated in the top 30 cm of the soil, as assumed in the CERES-Maize (Gabrielle and Kengni, 1996) and Century (Parton *et al.*, 1983) models. Following these assumptions, we set the number of soil layers (n_z) to two, thicknesses of top and bottom soil layers (d_{soil}) to thirty and forty centimeters, respectively, and root fraction (f_{root}) and optimum N mineralization rate (k_{min}) of the bottom soil layer to zero (Tables I and II). The forest floor was considered to be included in the top soil layer.

2.3.1. *N Mineralization*
It is assumed in SINIC that the quantity and quality of SOM does not change over the simulation period and that under optimal temperature and moisture conditions organic N would be mineralized at a fixed rate. This rate (k_{min}) in Equation (3) was

TABLE I

Parameters used in the hydrologic processes in SINIC to simulate streamflow at HBEF W6 during the period of 1964–1994

Name	Description	Used in	Value	Unit	Reference
n_z	Number of soil layers		2		Gabrielle and Kengni (1996); Parton *et al.* (1983)
L_{cell}	Cell length		363.32	m	HBEF web page[a]
$d_{soil}(1)$	Thickness of each soil layer		0.3	m	Federer (1995)
$d_{soil}(2)$			0.4		
$f_{root}(1)$	Fraction of water and nutrient absorbing roots in each soil layer	Equation (4)	1.0		Zollweg (1994)
$f_{root}(2)$			0.0		
Slope	Slope	Runoff processes	0.283		HBEF web page[a]
Z	Elevation	PET calculation	670.5	m	HBEF web page[a]
ϕ	Latitude	PET calculation	0.7667	radian	HBEF web page[a]
θ_{sat}	Soil water content at saturation	Equation (2)	0.6		Federer (1995)
θ_f	Soil water content at field capacity	Vertical water flux	0.25		Federer (1995)
θ_w	Soil water content at wilting point	Equation (2)	0.1		Campbell and Norman (1998)
K_{sat}	Saturated hydraulic conductivity	Vertical water flux	7.056×10^{-6}	m s^{-1}	Campbell and Norman (1998)
b	Exponent parameter for unsaturated hydraulic conductivity	Vertical water flux	4.9		Federer (1995)
I_{max}	Interception capacity of canopy surface	Surface processes	0.0015	m	Zollweg (1994)
R_{max}	Maximum retention capacity of soil surface	Surface processes	0.0025	m	Zollweg (1994)
$Slope_0$	Slope when no soil surface retention can occur	Surface processes	0.2		Zollweg (1994)
M_f	Melt factor	Snowmelt	4.75	mm $°C^{-1}$ per day	Gray and Prowse (1993)

(*Continued on next page*)

TABLE I
(*Continued*)

Name	Description	Used in	Value	Unit	Reference
CN	SCS curve number	Runoff processes	55		Rawls *et al.* (1993)
V_0^{land}	Land and stream runoff velocity when Slope = 1	Runoff processes	0.19	m s^{-1}	Zollweg (1994)
V_0^{stream}			2.25		
e_{in}	Exponent parameter for distributing infiltration water	Infiltration	0.3		Federer (1995)
r	Recession coefficient	Groundwater flux	0.2	per day	HBEF web page[a]
s	Seepage coefficient	Groundwater flux	0	per day	Federer (1995)
f_{sun}^{sunny}	Fraction of cloudless hours on sunny and rainy days	PET calculation	0.64		HBEF web page[a]
f_{sun}^{rainy}			0.16		
LAI_{max}	Maximum leaf area index	PET calculation	6		Federer (1995)
LAI_1	Day-of-year numbers describing changes in leaf area index	PET calculation	120		Federer (1995)
LAI_2			150		
LAI_3			260		
LAI_4			290		

[a]http://www.hubbardbrook.org/.

TABLE II

Parameters used in the nitrogen processes in SINIC to simulate streamflow NO_3^- loss from HBEF W6 during the period of 1964–1994

Name	Description	Used in	Value	Unit	Reference
κ	Soil thermal diffusivity	Soil temperature calculation	2.2×10^{-7}	$m^2\ s^{-1}$	Campbell and Norman (1998)
$n_{avg}(1)$	Number of days for averaging daily air temperature	Soil temperature calculation	7		Campbell and Norman (1998)
$n_{avg}(2)$			21		
Q_{10}	Factor change in rate with a 10 °C change in temperature	Equation (1)	3		Ross and Tate (1993); Godde *et al.* (1996)
T_b	Base temperature at which Q_{10} factor equals 1	Equation (1)	24	°C	Verchot *et al.* (2001)
$k_{min}(1)$	Daily net N Mineralization rate under optimal conditions	Equation (3)	0.36	g-N m^{-2} per day	Bohlen *et al.* (2001)
$k_{min}(2)$			0		
k_{nit}	Decay constant for nitrification	Equation (5)	0.05	per day	Vitousek *et al.* (1982)
k_{den}	Potential denitrification rate	Denitrification	0.1	g-N m^{-2} per day	Johnsson *et al.* (1987)
c_s	Half-saturation constant	Denitrification	10	mg-N L^{-1}	Johnsson *et al.* (1987)
θ_{den}	Threshold water content	Denitrification	0.5		Johnsson *et al.* (1987)
e_{den}	Exponent parameter for denitrification	Denitrification	2		Johnsson *et al.* (1987)
pH	Soil pH	Ammonia volatilization	4.24		Johnson *et al.* (1991)
R_1	Day-of-year numbers describing changes in plant N demand	Plant N uptake	85		Tierney *et al.* (2001)
R_2			180		
R_3			205		
R_4			305		
D_{year}	Annual plant N demand	Equation (4)	12.0	g-N m^{-2} per year	HBEF web page[a]

[a]http://www.hubbardbrook.org/.

obtained from a laboratory incubation study that reported the net N mineralization rates in the O_e horizon, O_a horizon, and upper 10 cm of mineral soil at HBEF averaged across four elevations (Bohlen *et al.*, 2001). The weighted k_{min} for the top soil layer (0.36 g-N m^{-2} per day) was calculated assuming uniform soil properties in the top 30 cm of mineral soil.

This optimal mineralization rate in situ is modified as the soil temperature and moisture conditions vary. The Q_{10} used to calculate the soil temperature factor (Equation (1)) was set to 3 following Ross and Tate (1993) and Godde *et al.* (1996). T_b, the room temperature at which the incubation study was performed, was set to 24 °C (Verchot *et al.*, 2001). The soil at HBEF has a sandy loam texture. The soil moisture contents at wilting point (θ_w) and at saturation (θ_{sat}) in Equation (2) were set to 0.1 from Campbell and Norman (1998) and 0.6 from Federer (1995), respectively.

2.3.2. *Nitrification*

The first-order decay constant for nitrification (k_{nit}) in Equation (5) was estimated using data reported in an incubation study performed by Vitousek *et al.* (1982), in which the weekly concentrations of NO_3^- and total inorganic nitrogen were reported throughout the entire eight-week incubation period, using samples from forest floor and mineral soil in the Hubbard Brook region. Because we are treating the forest floor and mineral soil as a single pool, nitrogen concentrations in these pools were aggregated to represent a single incubation study. The decay constant that gave the best fit to these aggregated data was determined to be 0.05 per day.

2.3.3. *Plant N Uptake*

It was assumed that the change in the relative size of daily plant N demand over time follows a similar pattern to the change in the daily new fine root growth over time. Tierney *et al.* (2001) measured the ratio of new fine root length to existing live fine root length in several plots at HBEF for two years. The new fine root growth started in late March, reached its maximum in early July, began to decline from late July, and fell to zero in late October. To reflect this pattern, day-of-year numbers for R_1, R_2, R_3, and R_4 (Table II) were set to 85, 180, 205, and 305, respectively.

The annual plant N demand (D_{year}) was calibrated so that the model reproduced the estimated average annual N uptake at HBEF W6 from 1964 to 1994. The average annual N uptake was estimated assuming that: (1) all of the leaves are lost with the N concentrations equal to what is measured in the litterfall and the same amount of N lost should be taken up next year, (2) the fine root production at HBEF in 1997 was 303 g m^{-2} per year (Tierney and Fahey, 2001) and the fine root production in any year can be estimated from the leaf biomass in that year relative to the leaf biomass in 1997, (3) annual N uptake in the woody tissue is the annual net change in wood biomass (net accumulation) times N concentration in the woody tissue, and (4) 0.535 g-N m^{-2} per year of nitrogen is taken up each year for growth of herbaceous species (Whittaker *et al.*, 1979). The tissue biomass

was estimated by linear interpolation from measurements taken in 1965, 1977, 1982, 1987, 1992, and 1997 (http://www.hubbardbrook.org/yale/vegetation/). Nitrogen concentrations in aboveground tissues were obtained from Whittaker *et al.* (1979). The species-weighted average N concentrations of fine roots (defined as <1 mm in diameter) and woody roots were calculated to be 1.73% and 0.42%, respectively, using data from Fahey *et al.* (1988) and Tierney and Fahey (2001).

Using this information, the average annual N uptake at HBEF W6 during the period of 1964 to 1994 was estimated to be 9.32 g-N m^{-2} per year. The model was run repeatedly with different values of D_{year}, until the simulated average annual N uptake yielded this estimate. The D_{year} is therefore not a 'free' parameter adjusted until NO_3^- export fits the measured data. It is adjusted until the simulated N uptake averaged over the entire simulation period matches the uptake estimated for the same period. The calibrated value of D_{year} was determined to be 12.0 g-N m^{-2} per year.

3. Results

3.1. Model evaluation

3.1.1. *Comparisons with Data*

SINIC successfully reproduced the observed high and low streamflow NO_3^- losses during the periods of high export (1968–1977) and low export (1978–1989), respectively, as well as four observed 'spikes' in 1970, 1973, 1976, and 1990 (calendar year) (Figure 2A). However, streamflow NO_3^- losses were overpredicted after the 1990 peak and in the low export period. The pattern in observed yearly streamflow was almost exactly reproduced by SINIC (Figure 2B). Box and whisker plots of simulated monthly NO_3^- losses over the 31 years studied (Figure 3A) reveal that SINIC reproduced the observed seasonal trend, and that the upward bias of the simulated NO_3^- loss was largely caused by overpredictions in the autumn and early winter. Predicted mean values were somewhat higher than observed in October-December, and also in May (Figure 3A). Corresponding monthly patterns of streamflow (Figure 3B) revealed that the predictions of monthly means matched observations well for each month of the year, and that the distributions of monthly streamflows for the period studied were well represented. The model overpredicted mean streamflow slightly in March and underpredicted somewhat in June, but the predictions for the other months were in better agreement.

All N pools (ammonium and nitrate) and fluxes (atmospheric deposition, mineralization, nitrification, plant uptake, denitrification, and ammonia volatilization) in SINIC showed highly significant positive correlations with measured streamflow NO_3^- loss (Table III). Correlations between streamflow NO_3^- and climatic

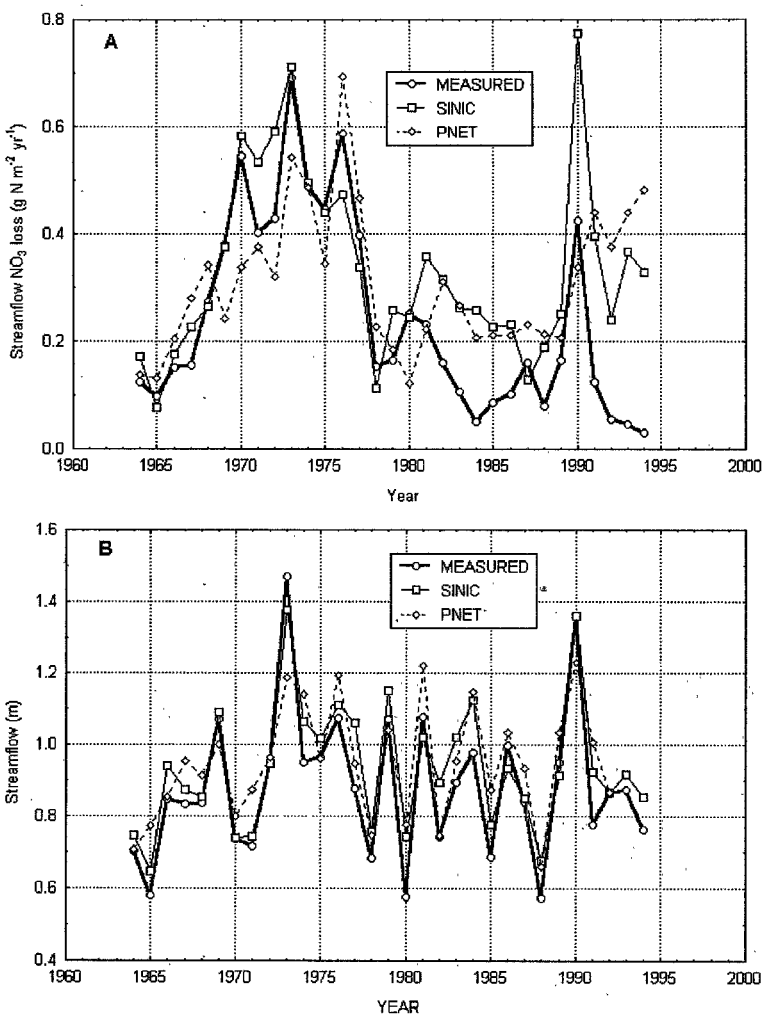

Figure 2. Comparisons of simulated annual streamflow NO_3^- loss (A) and streamflow (B) with measured values and predictions by PnET-CN, summarized on a calendar year basis. Streamflow NO_3^- loss predicted by PnET-CN (1964–1994) is from Aber and Driscoll (1997) and streamflow predicted by PnET-CN (1964–1992) is from Gbondo-Tugbawa *et al.* (2001).

variables were less strong, however, and air and soil temperatures, PET, AET, and soil water content were not significantly correlated to streamflow NO_3^-. However, the product of soil temperature and moisture factors showed a strong correlation with measured streamflow NO_3^- loss even though correlations with temperature and moisture factors were much weaker individually (Table III).

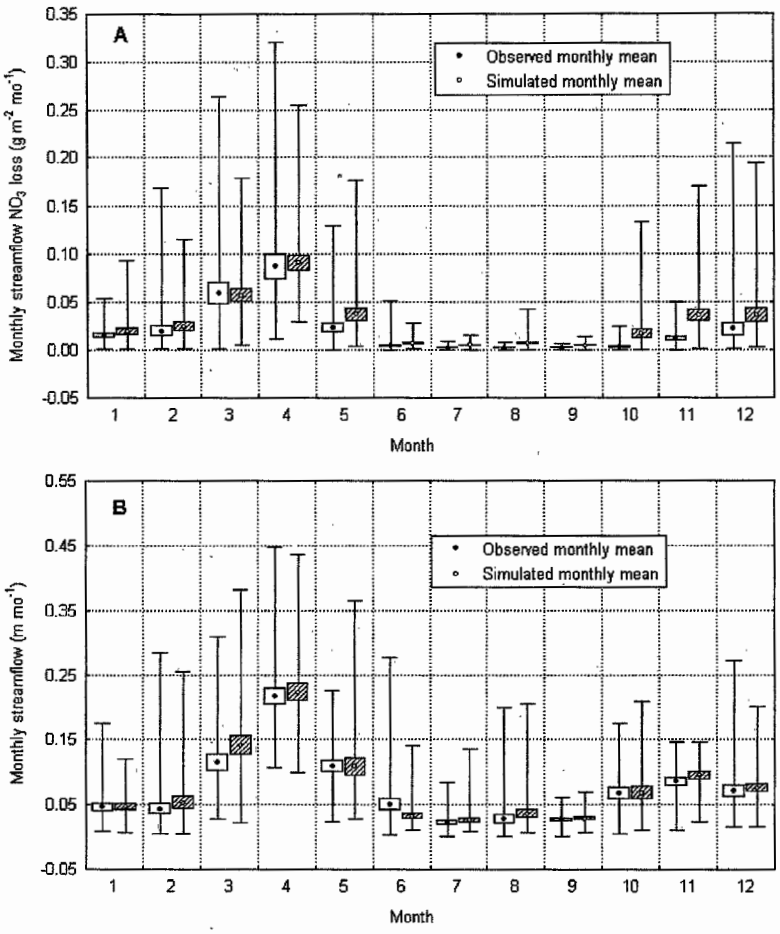

Figure 3. Box and whisker diagram, comparing monthly simulated and observed streamflow NO_3^- loss (A) and streamflow (B), showing the means, standard errors and extreme values over the 31-year period from 1964 to 1994.

3.1.2. *Comparisons with PnET-CN*

SINIC predictions of streamflow NO_3^- loss were compared with those of PnET-CN, a nitrogen model for forest catchments that has been applied to the Hubbard Brook watershed (Aber and Driscoll, 1997) and has led to conclusions that multiple disturbance events produced much of the N loss pattern (Aber *et al.*, 2002). Although both the PnET-CN and SINIC models reproduced the observed long-term pattern of streamflow NO_3^- loss from HBEF W6 for the 1964–1994 period well, SINIC was somewhat better in generating the four spikes as well as high NO_3^- export in

TABLE III

Mean, standard deviation, coefficient of variation (CV), and correlation coefficient (r) with measured streamflow NO_3^- loss of measured and simulated variables in SINIC for the entire simulation period (1964–1994). Variables are simulated unless indicated as 'measured'

Variable	Mean	Standard Deviation	CV	r	P-value
Measured streamflow NO_3^- loss (g-N m^{-2} per year)	0.244	0.182	0.746	1.00[c]	0
Streamflow NO_3^- loss simulated by SINIC (g-N m^{-2} per year)	0.335	0.171	0.510	0.78[c]	1.8×10^{-7}
Streamflow NO_3^- loss simulated by PnET-CN (g-N m^{-2} per year)[a]	0.310	0.134	0.431	0.55[c]	0.0014
Measured streamflow (m per year)	0.881	0.204	0.232	0.52[c]	0.0025
Streamflow simulated by SINIC (m per year)	0.935	0.178	0.191	0.48[c]	0.0062
Streamflow simulated by PnET-CN (1964–1992 period) (m per year)[b]	0.950	0.159	0.168	0.42[c]	0.022
Atmospheric N input (g-N m^{-2} per year)	0.739	0.120	0.163	0.58[c]	7.1×10^{-4}
Atmospheric N input as rainfall N + dry deposition (g-N m^{-2} per year)	0.507	0.104	0.206	0.42[c]	0.017
Atmospheric N input as snowmelt N (g-N m^{-2} per year)	0.232	0.054	0.231	0.46[c]	0.0085
N mineralization (g-N m^{-2} per year)	8.925	1.790	0.201	0.52[c]	0.0027
Nitrification (g-N m^{-2} per year)	0.438	0.330	0.753	0.66[c]	5.1×10^{-5}
Soil NH_4^+ concentration (g-N m^{-3} soil)	1.786	1.047	0.586	0.73[c]	2.6×10^{-6}
Soil NO_3^- concentration (g-N m^{-3} soil)	0.190	0.125	0.659	0.73[c]	3.9×10^{-6}
Soil inorganic N concentration (g-N m^{-3} soil)	1.976	1.164	0.589	0.74[c]	2.1×10^{-6}
Plant N uptake (g-N m^{-2} per year)	9.325	1.587	0.170	0.52[c]	0.0028
Plant NH_4^+ uptake (g-N m^{-2} per year)	8.709	1.411	0.162	0.49[c]	0.0054
Plant NO_3^- uptake (g-N m^{-2} per year)	0.617	0.229	0.372	0.58[c]	5.7×10^{-4}
Denitrification (g-N m^{-2} per year)	0.0010	0.00051	0.494	0.78[c]	2.0×10^{-7}
NH_3 volatilization (g-N m^{-2} per year)	1.4×10^{-5}	8.9×10^{-6}	0.635	0.73[c]	3.0×10^{-6}

(*Continued on next page*)

TABLE III
(*Continued*)

Variable	Mean	Standard Deviation	CV	r	P-value
N mineralization – plant N uptake (g-N m^{-2} per year)	−0.401	0.583	−1.454	0.19	0.31
Nitrification – plant NO_3^- uptake (g-N m^{-2} per year)	−0.179	0.144	−0.802	0.59[c]	5.4×10^{-4}
Nitrification + atmospheric N input – plant NO_3^- uptake (g-N m^{-2} per year)	0.560	0.219	0.391	0.70[c]	1.2×10^{-5}
Temperature factor	0.088	0.010	0.108	0.36[c]	0.050
Moisture factor	0.928	0.051	0.055	0.31	0.088
Temperature factor × moisture factor	0.067	0.013	0.200	0.52[c]	0.0026
Measured air temperature (°C)	4.136	0.586	0.142	0.28	0.13
Soil temperature (°C)	6.692	0.344	0.051	0.33	0.070
Measured precipitation (rainfall + snowfall) (m per year)	1.405	0.188	0.134	0.51[c]	0.0034
Water input as rainfall + snowmelt (m/yr)	1.405	0.211	0.150	0.50[c]	0.0044
Measured rainfall (m per year)	0.952	0.179	0.188	0.37[c]	0.041
Snowmelt (m per year)	0.453	0.096	0.211	0.41[c]	0.024
PET (m per year)	0.634	0.068	0.107	0.07	0.72
AET (m per year)	0.381	0.042	0.110	0.30	0.10
Soil water content (m^3 water m^{-3} soil)	0.288	0.017	0.058	0.27	0.14

[a]From Aber and Driscoll (1997).
[b]From Gbondo-Tugbawa *et al.* (2001).
[c]Correlation coefficients exhibiting significant differences from zero at the 95% level.

TABLE IV

Statistical comparisons of predictions by SINIC and PnET-CN to observations.

		r-square	NMSE[a]	NME[b]
Annual streamflow NO_3^- loss (1964–1994)	SINIC	0.61	0.67	0.37
	PnET-CN[c]	0.30	0.87	0.27
Annual streamflow (1964–1992)	SINIC	0.89	0.18	0.06
	PnET-CN[d]	0.74	0.37	0.08
Monthly streamflow NO_3^- loss (1964–1994)	SINIC	0.61	0.44	0.37
Monthly streamflow (1964–1992)	SINIC	0.85	0.17	0.06

Published monthly PnET-CN predictions were not available.

[a]Normalized Mean Square Error = $\Sigma(o_i - p_i)^2/\Sigma(o_i - \bar{o})^2$, where o_i is the ith observation, p_i is the ith prediction, and $\bar{o}$ is the mean of the observations; NMSE = 0 indicates perfect agreement; NMSE = 1 occurs if the mean of the observations is used as the predictor (values of NMSE of one or greater indicate that the modeled values would be better substituted by the mean of the observations).

[b]Normalized Mean Error = bias (mean of differences between the observed and predicted values) divided by mean of observed values; NME = 0 indicates perfect agreement; NME = 1 shows the predictor is biased upward from the observations by 100% on average.

[c]From Aber and Driscoll (1997).

[d]From Gbondo-Tugbawa *et al.* (2001).

high years (Figure 2A). As a result, the r^2 value for yearly streamflow NO_3^- loss was much higher in SINIC (0.61) than in PnET-CN (0.30), indicating that SINIC explained a higher proportion of the NO_3^- export pattern observed at HBEF W6 (Table IV). Both PnET-CN and SINIC overpredicted the NO_3^- export after 1990 and in the low period (Figure 2A).

Published yearly streamflow predictions are not available for PnET-CN. Instead, yearly streamflow predictions by PnET-BGC, in which a submodel of biogeochemical cycling of other elements is added to PnET-CN (Gbondo-Tugbawa *et al.*, 2001), were compared with SINIC simulations over the 1964–1992 period. The PnET-BGC and PnET-CN produce identical results for hydrology (S. Gbondo-Tugbawa, personal communication). Measured yearly streamflow was closely reproduced by both SINIC and PnET (Figure 2B), except for some slight deviations observed in PnET predictions, which probably lowered the r^2 value relative to SINIC predictions (Table IV). Normalized mean square error (NMSE) values for NO_3^- loss and streamflow were smaller in SINIC, indicating that SINIC predictions produced smaller deviations from observed values overall (Table IV). All normalized mean error (NME) values were positive, and the NME for streamflow NO_3^- loss was higher in SINIC. Thus N export was overpredicted (i.e. biased upward) in SINIC more than in PnET-CN. Both models slightly overpredicted streamflow as well. Monthly statistics in SINIC were similar to yearly statistics (Table IV).

3.2. Comparisons between the periods of high and low streamflow NO_3^- loss

3.2.1. *Results of t-Tests*

As shown in Table V, measured annual NO_3^- loss was significantly higher during the 1968–1977 period than the 1978–1989 period, although there was no difference in measured streamflow. SINIC successfully predicted this difference in streamflow NO_3^- loss between two periods. Atmospheric N input was significantly higher in the high streamflow NO_3^- loss period than in the low period. When the components of atmospheric N input, including wet and dry deposition and snowmelt N, were analyzed separately, only the snowmelt N showed a significant difference (P-value = 0.0018). Snowmelt was also higher in the high period, although the difference was not as highly significant as was snowmelt N (P-value = 0.041). The measured air temperature, simulated soil temperature, and soil moisture content were not significantly different between two periods. While the temperature and moisture factors were not significantly different between the two periods when analyzed separately, the product of the soil temperature and moisture factors was significantly higher in the high period. As a result of the difference in the combined effect of soil temperature and moisture, simulated N mineralization, a function of these factors only, was predicted to be greater during the high period as well. All simulated nitrogen pools (ammonium and nitrate) and fluxes (nitrification, plant uptake, denitrification, and ammonia volatilization) were also higher in the high streamflow NO_3^- loss period than in the low period. Nitrogen mineralization minus plant N uptake was less negative in the high period, indicating higher soil N availability, but the difference between the two periods was not significant because of the large variation.

3.2.2. *Reciprocal Replacement of Time Series (RRTS) Analysis*

The response of NO_3^- loss in streamflow to temporal pattern of one or more driving variables was evaluated by interchanging (i.e. 'reciprocally replacing') a decadal time series of driving variables between the high streamflow NO_3^- loss years (1968–1977) and the last decade of the low years (1980–1989) (Figure 4). Both periods were chosen to be 10 years long, and to begin in leap years for analytical convenience (exact matching of the period lengths). The driving variables selected for analysis include four climatic variables (precipitation, PET, soil temperature, and N deposition) that together determine the pattern of simulated streamflow NO_3^- loss in SINIC, and nitrogen input to the system as N deposition and N mineralization. We replaced the daily data for these variables for 1968–77 with the data from 1980-1989 and vice versa to test the influence of the pattern of these driving variables on model behavior.

When these four climatic driving variables were interchanged, the pattern of 10 years of NO_3^- loss was exchanged exactly, including three spikes in the high period (Figure 4, case a), confirming that SINIC predicts long-term N export pattern strictly

TABLE V

Comparison of measured and simulated variables in SINIC between the period of high streamflow NO_3^- loss (1968–1977) and the low period (1978–1989)

Variable	Mean 1968–1977	Mean 1978–1989	Std Dev 1968–1977	Std Dev 1978–1989	*P*-value
Measured streamflow NO_3^- loss (g-N m^{-2} per year)[c]	0.464	0.142	0.118	0.060	7.3×10^{-8}
Streamflow NO_3^- loss simulated by SINIC (g-N m^{-2} per year)[c]	0.481	0.236	0.133	0.069	1.9×10^{-5}
Streamflow NO_3^- loss simulated by PnET-CN (g-N m^{-2} per year)[ac]	0.415	0.218	0.133	0.045	9.4×10^{-5}
Measured streamflow (m per year)	0.964	0.839	0.215	0.182	0.16
Streamflow simulated by SINIC (m per year)	1.000	0.904	0.191	0.152	0.21
Streamflow simulated by PnET-CN (m per year)[b]	0.998	0.931	0.134	0.173	0.33
Atmospheric N input (g-N m^{-2} per year)[c]	0.804	0.691	0.095	0.077	0.0058
Atmospheric N input as rainfall N + dry deposition (g-N m^{-2} per year)	0.533	0.490	0.104	0.075	0.27
Atmospheric N input as snowmelt N (g-N m^{-2} per year)[c]	0.271	0.202	0.053	0.038	0.0018
N mineralization (g-N m^{-2} per year)[c]	9.881	8.139	1.655	1.838	0.031
Nitrification (g-N m^{-2} per year)[c]	0.679	0.282	0.324	0.237	0.0035
Soil NH_4^+ concentration (g-N m^{-3} soil)[c]	2.783	1.107	0.965	0.422	2.5×10^{-5}
Soil NO_3^- concentration (g-N m^{-3} soil)[c]	0.305	0.119	0.134	0.049	0.00023
Soil inorganic N concentration (g-N m^{-3} soil)[c]	3.089	1.227	1.089	0.457	2.8×10^{-5}
Plant N uptake (g-N m^{-2} per year)[c]	10.23	8.560	1.543	1.568	0.021
Plant NH_4^+ uptake (g-N m^{-2} per year)[c]	9.47	8.03	1.37	1.43	0.026
Plant NO_3^- uptake (g-N m^{-2} per year)[c]	0.77	0.53	0.23	0.19	0.017
Denitrification (g-N m^{-2} per year)[c]	0.0015	0.00073	0.00040	0.00021	2.7×10^{-5}
NH_3 volatilization (g-N m^{-2} per year)[c]	2.2×10^{-6}	8.8×10^{-6}	8.4×10^{-6}	4.4×10^{-6}	0.00013
N mineralization – plant N uptake (g-N m^{-2} per year)	−0.353	−0.422	0.557	0.489	0.76
Nitrification – plant NO_3^- uptake (g-N m^{-2} per year)[c]	−0.086	−0.252	0.156	0.077	0.004

(*Continued on next page*)

TABLE V
(*Continued*)

Variable	Mean 1968–1977	Mean 1978–1989	Std Dev 1968–1977	Std Dev 1978–1989	*P*-value
Nitrification + atmospheric N input - plant NO_3^- uptake (g-N m^{-2} per year)[c]	0.718	0.440	0.187	0.104	0.0003
Temperature factor	0.092	0.089	0.010	0.0094	0.42
Moisture factor	0.941	0.912	0.060	0.052	0.24
Temperature factor × moisture factor[c]	0.075	0.062	0.012	0.014	0.031
Measured air temperature (°C)	4.271	4.007	0.609	0.563	0.30
Soil temperature (°C)	6.812	6.675	0.397	0.280	0.35
Measured precipitation (rainfall + snowfall) (m per year)	1.482	1.376	0.165	0.199	0.19
Water input as rainfall + snowmelt (m/yr)	1.484	1.375	0.207	0.190	0.21
Measured rainfall (m per year)	0.974	0.951	0.188	0.185	0.78
Snowmelt (m per year)[c]	0.510	0.424	0.074	0.106	0.041
PET (m per year)	0.643	0.638	0.113	0.026	0.89
AET (m per year)	0.390	0.383	0.037	0.054	0.72
Soil water content (m^3 water m^{-3} soil)	0.289	0.283	0.020	0.016	0.43

Variables are simulated unless indicated as 'measured'.
[a]From Aber and Driscoll (1997).
[b]From Gbondo-Tugbawa *et al.* (2001).
[c]Variables exhibiting significant differences in their mean annual values between these periods at 95% level.

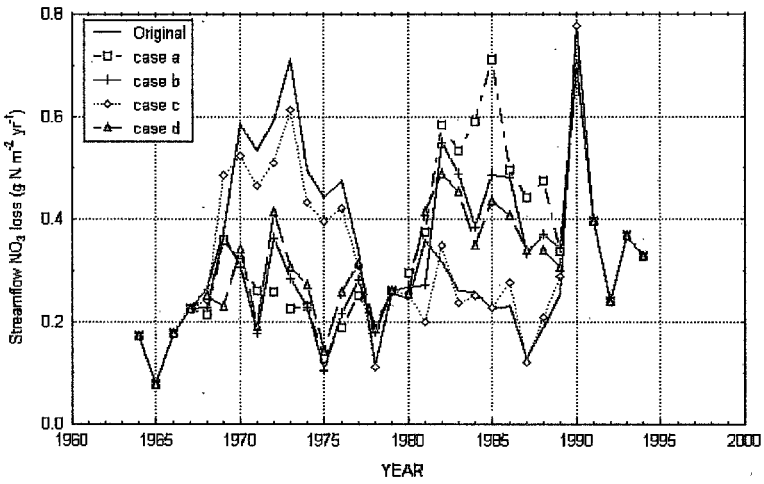

Figure 4. RRTS analysis of simulated streamflow NO_3^- loss from HBEF W6, with the time series of driving variables swapped between two 10-year periods of 1968–1977 and 1980–1989; case a: four climatic variables (precipitation, PET, soil temperature, and N deposition) swapped; case b: N deposition and f_T (temperature factor) $\times$ f_M (moisture factor) for N mineralization swapped; case c: N deposition swapped; case d: $f_T \times f_M$ for N mineralization swapped.

based on year-to-year climatic variability. When inorganic nitrogen input to the soil (atmospheric N input plus N mineralization) was interchanged between two periods (Figure 4, case b), the pattern was similarly reversed, although differences between the two periods were diminished and the second spike originally observed in 1973 was reduced significantly. Interchanging atmospheric N input alone (Figure 4, case c) had almost no effect in changing the pattern, although the heights of three spikes in the high period were decreased slightly. The pattern of NO_3^- loss simulated after interchanging N mineralization was almost identical to that obtained when total N input to the soil was interchanged (Figure 4, case d), suggesting that N mineralization, not N deposition, was the actual driver for creating the observed long-term pattern of N export from HBEF W6.

4. Discussion

4.1. Model evaluation

SINIC reproduced significant features of the long-term pattern of NO_3^- export from HBEF W6, including four spikes in 1970, 1973, 1976, and 1990, as well as decadal trends of high streamflow NO_3^- flux in 1968–1977 and low flux in 1978-1989 (Figure 2A). Because SINIC does not include soil freezing, insect defoliation, and long term effects of drought, we cannot evaluate their roles directly. However, the

SINIC simulation did explain a large proportion of the long-term N export pattern in HBEF W6, suggesting that annual variations as well as long-term trends observed in this watershed may have resulted from variations in soil N mineralization driven by simple climatic variation. For example, the two spikes of NO_3^- export in 1990 and in 1973, which have been attributed to soil freezing events during winter periods (Mitchell *et al.*, 1996; Likens and Bormann, 1995), may have been associated with high annual temperature (Figure 5A) and precipitation (Figure 5B) which occurred

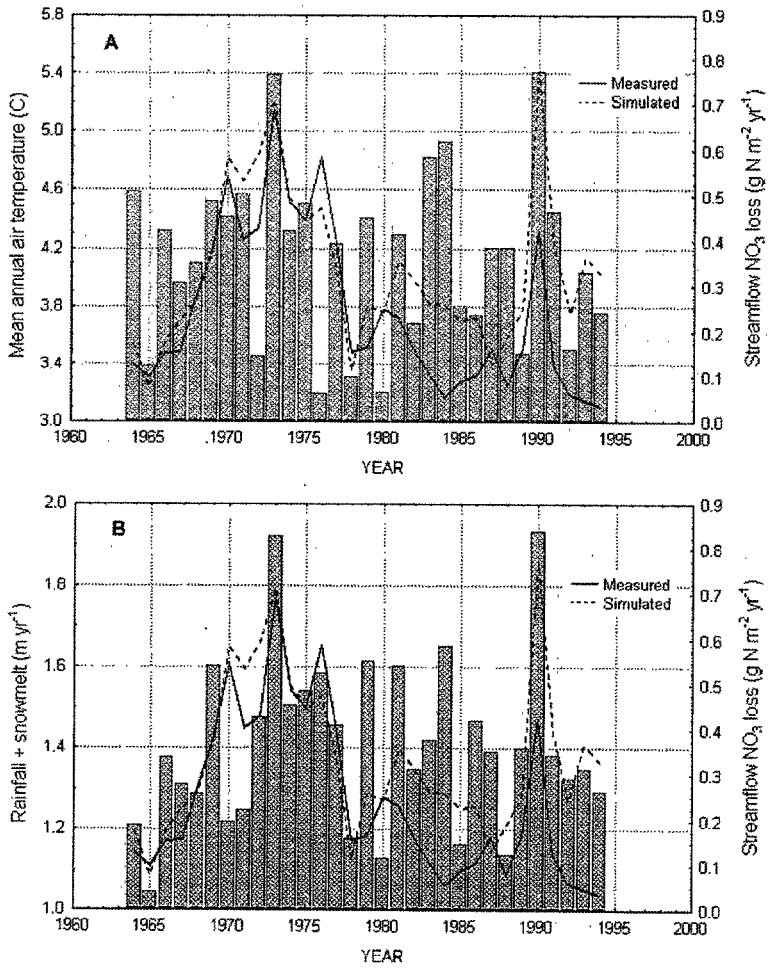

Figure 5. Annual streamflow NO_3^- loss from HBEF W6 and mean air temperature (A) and water input to the soil (B) during 1964–1994 period.

simultaneously in those years. The potential of insect defoliation and drought to generate a large amount of N export was questioned by Lovett *et al.* (1998) and Tietema *et al.* (1997), respectively. The assumption in SINIC that yearly plant N uptake potential is constant for all years and was not disrupted by events such as soil freezing, insect defoliation, and drought did not prevent the model from predicting the year-to-year fluctuations in streamflow NO_3^- flux.

A key assumption in SINIC is that there had been little change in the size and chemical properties of SOM during the simulation period, which permits mineralization to be represented as a zeroth-order process with respect to the SOM pool, dependent upon soil temperature and moisture only. Even the most extreme form of forest disturbance, the clearcutting of HBEF W5, did not change the SOM pool size (Huntington and Ryan, 1990) nor its chemistry (Dai *et al.*, 2001) significantly. The only part of the SOM that shows large variation in a relatively short time period is the aboveground forest floor. Many nitrogen cycle models such as TRACE (Currie and Nadelhoffer, 1999), Century (Parton *et al.*, 1993), and FORTNITE (Aber *et al.*, 1982) include detailed submodels of SOM with more than one pool for the aboveground forest floor. However, Aber *et al.* (1997) reported that these pools had little control on overall N dynamics and may well be aggregated into the SOM pool. In field studies, litter removal did not have significant effects on microbial activities (Fisk and Fahey, 2001) and aboveground responses (Fahey *et al.*, 1998), suggesting that its effect on N dynamics may be buffered by the much larger belowground SOM pool, which has a greater control of soil nutrient cycling (Fisk and Fahey, 2001). Under the assumption of a relatively constant SOM pool, soil N dynamics such as N mineralization rates may be predicted by modifying the results of a standardized laboratory incubation study, as a function of soil temperature and moisture (Schmidt, 1982). A close match between N dynamics obtained from laboratory incubation and field measurements has been demonstrated previously, suggesting that laboratory incubation is a good way of estimating the *in situ* N cycling rates (Ollinger *et al.*, 2002; Verchot *et al.*, 2001).

Despite these observations, we acknowledge that the assumption of a relatively unchanging SOM pool may be overly simplistic, and may be responsible for some deviations from observations in the SINIC simulation results. The degree of overprediction gradually increased from the 1980s and became substantial after 1990 (Figure 2A), suggesting that there may have been a gradual change in the SOM pool throughout the simulation period. It is not clear why SINIC overpredicted nitrate loss in the later period of simulation. Some studies suggested that net N mineralization rate may decrease with time as microbial demand for inorganic nitrogen increases because of accumulation of detrital biomass in the forest (Fisk *et al.*, 2002) and higher rates of microbial turnover and N immobilization (Fisk and Fahey, 2001; Aber *et al.*, 1998). However, it is generally recognized that older forests are expected to have higher rates of N loss (Goodale *et al.*, 2000; Goodale and Aber, 2001) due to higher N mineralization and lower plant N uptake (Vitousek *et al.*, 1989; Aber *et al.*, 1989). In any case, this forest clearly has not entered the

stage when demand is greatly exceeded by mineralization, and SINIC seems to be overestimating mineralization in the later period of simulation. As noted above, changes in plant and SOM pools are not explicitly calculated in SINIC, which makes the model inappropriate for simulating nitrogen dynamics over centuries when significant changes in plant and SOM pools are to be expected (Parton *et al.*, 1983). However, to keep the model as simple as possible, no additional processes were introduced to improve the fit over the latter, relatively small, portion of the data record. The model simulates N flux during the periods of 1968–1977 and 1978–1989 well enough that it can be used as a tool to investigate the differences between these two periods.

4.2. PROCESSES CONTROLLING THE LONG-TERM PATTERN OF NO_3^- EXPORT

It is surprising that most variables in SINIC, summarized on a yearly basis, were positively correlated with measured streamflow NO_3^- loss (Table III). Such dependencies among flux variables make it difficult to determine which factors control the pattern of nitrogen export using only correlation or regression analyses (Murdoch *et al.*, 1998; Williard *et al.*, 1997; Kortelainen *et al.*, 1997). Comparisons between the periods of high (1968–1977) and low (1978–1989) streamflow NO_3^- loss (Table V) suggest that inorganic nitrogen input to the soil, both as deposition and mineralization, was significantly higher in the high period. As a result, soil nitrogen availability and all N fluxes limited by nitrogen availability (nitrification, plant uptake, denitrification, and ammonia volatilization), as well as N export, were significantly higher in the period of high streamflow NO_3^- loss. Since the difference in mineralization between the high and low periods was more than 10 times higher than the difference in atmospheric N input (1.742 g-N m^{-2} per year vs. 0.113 g-N m^{-2} per year), it can be surmised that N mineralization was more important in controlling NO_3^- export from HBEF W6. This conclusion is supported by the RRTS analysis (Figure 4), which demonstrated that replacing the time series of atmospheric N deposition between the high and low periods had almost no effect on the long-term pattern of NO_3^- export, whereas replacing the time series of N mineralization almost reversed the pattern. The results of RRTS analysis indicate that the positive correlation between N deposition and streamflow N should not be interpreted as a cause-effect relationship.

Nitrate loss was not uniformly distributed over the year. Summertime losses were negligible, some losses occurred during the fall, but the greatest losses occurred during the late winter and spring runoff (Figure 3A). The biggest monthly difference in nitrate outflow between the high and low periods usually occurred during spring runoff period (average of maximum monthly loss is 0.2 g-N m^{-2} mo^{-1} $\pm$ 0.06 during 1968–1977 compared to 0.075 g-N m^{-2} mo^{-1} $\pm$ 0.05 during 1978–1989, a difference of approximately 0.12 g-N m^{-2} mo^{-1}). The peak month averages 42% of the annual measured loss during the high flux period, and 49%, during the low period. Nitrate loss showed significant differences between two periods

in all months except January and February. Differences in monthly atmospheric N input were relatively weak, appearing only at the 90% level in April, May and July. The product of soil temperature and moisture factors, and thus simulated N mineralization, were significantly different in May, July, September and October. Over the eight months preceding the peak month of spring outflow, simulated cumulative differences in mineralization between the high and low periods averaged 1.5 g-N m^{-2}, cumulative differences in nitrification averaged 0.37 g-N m^{-2}. These processes led to a cumulative difference between the two periods of 0.12 g-N m^{-3} in the soil NO_3^- pool over the same 8 months, and a 0.11 g-N m^{-3} difference in soil NO_3^- concentration during the peak spring outflow month. Consequently, the difference in nitrate lost between the high and low periods during the peak month is equivalent to one third of difference in the nitrate generated during the previous 8 months. The seasonal pattern appears to be that while some nitrate leaks from the watershed during the fall and winter months, it generally accumulates in the soil until there is sufficient water to flush it out during the thaws of the following spring.

For the mineralized ammonium to be exported from a watershed with streamflow, it must be nitrified to nitrate, which has much higher mobility in the soil than ammonium (Vitousek and Melillo, 1979). Thus nitrification is referred to as a 'gatekeeper' for nitrogen losses (Robertson, 1982). High nitrification potential has been related to high stream NO_3^- in two experimental watersheds in West Virginia (Christ *et al.*, 2002). Isotopic tracer studies have revealed that stream NO_3^- originates from nitrification, not directly from atmospheric deposition (Mayer *et al.*, 2002; Nadelhoffer *et al.*, 1999). In our study, measured annual NO_3^- export was more strongly correlated with nitrification than with N mineralization (Table III), and the difference between the high and low periods of streamflow NO_3^- loss was more significant for nitrification than for N mineralization (Table V). These observations suggest that nitrification, rather than N mineralization, may have played a key role in controlling the pattern of N loss from HBEF W6.

To investigate the relative importance of various processes on the control of nitrate loss, we performed a series of additional RRTS analyses (Figure 6). Nitrification is calculated in SINIC as a function of the product of soil temperature and moisture factors and soil NH_4^+ availability (Equation (5)). When the time series of the modifying factors (the product of temperature and moisture factors) for nitrification was reciprocally replaced, little change occurred in the long-term pattern of simulated NO_3^- export (Figure 6, case a). The pattern was almost reversed, however, when the time series of modifying factors both for N mineralization and nitrification were replaced (Figure 6, case b). The additional reciprocal replacement of atmospheric N deposition showed only a minor contribution to the pattern (Figure 6, case c). Reciprocal replacement of atmospheric N deposition and nitrification together did not change the NO_3^- export pattern significantly (Figure 6, case d), suggesting that NH_4^+ supply from atmospheric deposition is not the dominant source for nitrification. Based on these analyses, we conclude that the rate of nitrification is heavily dependent upon availability of soil ammonium supplied by

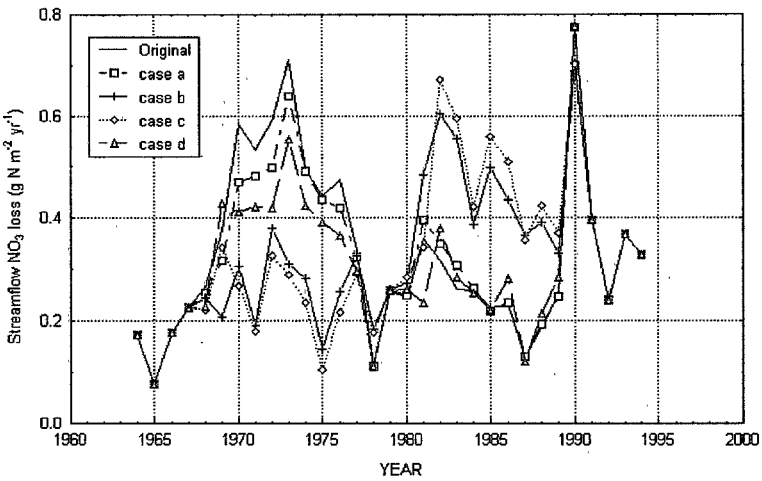

Figure 6. RRTS analysis of simulated streamflow NO_3^- loss from HBEF W6, with the time series of driving variables swapped between two 10-year periods of 1968–1977 and 1980–1989; case a: f_T (temperature factor) × f_M (moisture factor) for nitrification swapped; case b: $f_T \times f_M$ for N mineralization and nitrification swapped; case c: N deposition and $f_T \times f_M$ for N mineralization and nitrification swapped; case d: N deposition and $f_T \times f_M$ for nitrification swapped.

mineralization. The apparent temperature and moisture dependence of nitrification rate lies in the direct effects of these factors on N mineralization, the source of the ammonium pool. The importance of soil NH_4^+ mineralized from organic matter in controlling the rates of nitrification has been discussed by Rosswall (1982), Robertson and Vitousek (1981), and Gbondo-Tugbawa and Driscoll (2002). In a soil incubation study at HBEF, N mineralization rates and stream NO_3^- concentrations showed the same increasing trend with increasing elevation (Bohlen *et al.*, 2001). Watersheds in the mid-Appalachian region with high, medium, and low N mineralization rates showed high, medium, and low nitrification rates and NO_3^- leaching, respectively (Williard *et al.*, 1997). Links between N mineralization rate, soil NO_3^- pool, and NO_3^- leaching loss were demonstrated in northern hardwood forests in western Upper Michigan (Fisk *et al.*, 2002).

In SINIC, daily variation in the product of soil temperature and moisture factors is the only determinant of the daily N mineralization. If N mineralization has exerted an important influence on N dynamics and streamflow NO_3^- flux at HBEF W6, this product must have followed a similar pattern. Indeed, a nonlinear fit of the average product of the daily temperature factor and moisture factor to a simple function of time, such as a linear trend plus a damped sine term (to remove the higher frequency components of the time series) exhibits a long-term pattern roughly similar to that observed in streamflow NO_3^-, with a large peak in the 1970s, a large valley in the 1980s, and a smaller peak around 1990 (Figure 7).

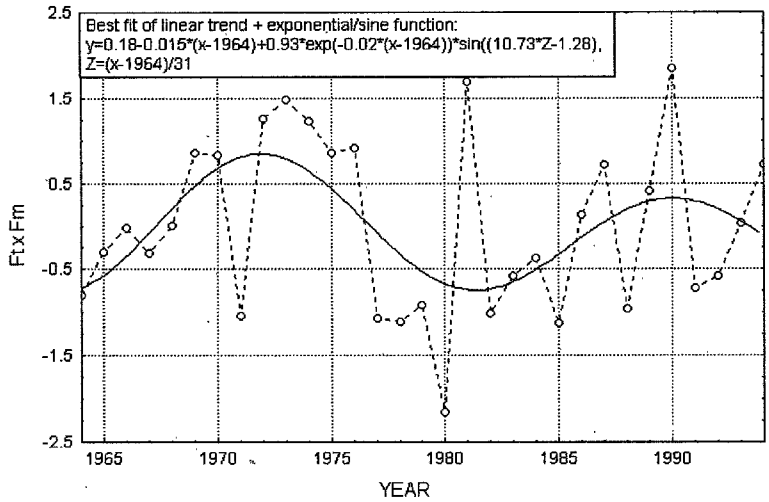

Figure 7. Yearly standardized (mean subtracted and divided by standard deviation) f_T (temperature factor) $\times f_M$ (moisture factor). The solid line is the nonlinear fit of a linear trend plus exponential/sine function.

Therefore, we conclude that changes over time in the interaction of temperature and moisture factors on N mineralization produced the shifts in long-term streamflow NO_3^- loss simulated in SINIC and possibly in the NO_3^- export patterns observed at HBEF W6 as well. Neither the temperature factor nor the moisture factor alone displayed this pattern. Although the product of the temperature factor and moisture factor was significantly higher in the high NO_3^- export period than in the low period, these individual factors were not significantly different between two periods (Table V). Climatic variables that are used to calculate the temperature factor (air and soil temperatures) and the moisture factor (precipitation and PET) also did not show significant differences. Longer term climatic record (1956–2003) available at HBEF W1, which is close to W6, did not suggest any long term trend in precipitation and air temperature that could explain the difference in NO_3^- export between two periods (http://www.hubbardbrook.org/research/data/data.htm). The climatic variables in these periods did not seem to deviate from average long term climatic condition. Although Murdoch *et al.* (1998) reported that mean air temperature alone was significantly correlated with N export at the Biscuit Brook watershed in the Catskill Mountains, NY, this was not the case at HBEF W6 (Table III). Thus, while the cumulative interaction of climatic factors was sufficient to explain most features of the long-term pattern of streamflow NO_3^- loss from this watershed, this relationship would not have been revealed by examining individual climatic variables. We believe that this study illustrates the value of a modeling approach, together with carefully constructed assumptions and proper

'probing' tools such as RRTS analysis, for evaluating the interactive effects of interannual climatic variability on soil N dynamics and NO_3^- losses from forested ecosystems.

4.3. Missing processes

How likely is it that processes omitted from these simulations, such as disturbance, N fixation, and abiotic immobilization could indirectly have played a role in causing the difference in NO_3^- export between the two periods? In SINIC, the initial state of the system is embedded in several parameters including k_{min} (daily net N mineralization rate under optimal conditions; Equation (3)) and D_{year} (annual plant N demand; Equation (4)). The exact values of these parameters may reflect the disturbance history of the watershed being modeled, and may be an integration of many site-specific properties such as C:N ratio (Ollinger *et al.*, 2002; Kortelainen *et al.*, 1997), site fertility (Williard *et al.*, 1997), soil pH (Christ *et al.*, 2002), species composition (Lovett *et al.*, 2000), and topographic features (Bohlen *et al.*, 2001). The applicability of SINIC to other watersheds may be limited by data availability, because estimating k_{min} and D_{year} requires data from soil incubation study and forest inventory, respectively. Spatial and temporal variation in potential mineralization rate observed in soil incubation studies (Bohlen *et al.*, 2001) may also make the estimation of k_{min} difficult.

SINIC does not include some nitrogen cycling processes such as N fixation and abiotic immobilization of inorganic N into SOM. Nitrogen fixation at HBEF W6 has been estimated to be as high as 1.42 g-N m^{-2} per year, although this value is obtained by difference from balancing the N budget (Bormann *et al.*, 1977). Abiotic immobilization may play an important role in N retention in forested ecosystems, but quantitative description of this process has not been accomplished yet (Dail *et al.*, 2001; Aber *et al.*, 1998). SINIC also does not include all components of streamflow N export. Dissolved organic nitrogen (DON) was a major component of streamflow N loss from forested watersheds in the northeastern United States including HBEF W6 (Campbell *et al.*, 2000), and it is known that DON and ammonium can be the dominant forms of N in pristine forest streams (Perakis and Hedin, 2002). However, despite the prominent role that has been identified for these processes under specific conditions, there is no reason to suspect that their addition to the model would improve its predictive ability, and there is no obvious reason why changes in these processes between the two periods would result in the differences in NO_3^- loss. We have shown that a relatively simple nitrogen cycle model was able to reproduce most of the multi-decadal pattern of N export from HBEF W6 without considering the effects of extreme events on soil N dynamics. Nitrogen mineralization was the most likely driver for the long-term pattern. Although nitrification is an important process generating the soil NO_3^- pool, the supply of ammonium from N mineralization drives the nitrification rate. Because the interaction of soil temperature and moisture is the only determinant of the N mineralization rate in SINIC, we

conclude that these factors produced the shifts in long-term NO_3^- export simulated in our model and likely those observed at HBEF W6. These results are important because they differ from previous analyses, which have ascribed the pattern of N loss to a complex of processes including soil freezing and insect defoliation that are difficult to measure or predict accurately, and to delayed effects of drought or hurricane damage over multiple decades. In contrast to these earlier reports, our results suggest that the interaction of daily temperature and moisture effects, without significant lag periods, plays a dominant role in predicting the observed pattern of NO_3^- export.

Acknowledgements

This research was funded by the United States Environmental Protection Agency (EPA) High Performance Computing program, grant number: R 825208-01-0. Additional support was provided by an educational support grant to Boyce Thompson Institute from the Alcoa Foundation and the National Science Foundation. The U.S. Department of Agriculture Forest Service, Northeastern Research Station, Project NE-4104 provided partial support for Dr. Woodbury's participation. The sponsors of this research have not formally reviewed this document and it should not be construed to represent their policies. Some data used in this publication was obtained by scientists of the Hubbard Brook Ecosystem Study; this publication has not been reviewed by those scientists. The precipitation and streamwater chemistry data were provided by Gene E. Likens through funding by the National Science Foundation and the A. W. Mellon Foundation. The Hubbard Brook Experimental Forest is operated and maintained by the Northeastern Research Station, U.S. Department of Agriculture, Newtown Square, Pennsylvania. Our sincere thanks also go to two anonymous reviewers, Dr. Timothy Fahey for his review of an earlier draft of the manuscript, and Dr. Gary Lovett for helpful discussions.

References

Aber, J. D., Ollinger, S. V., Driscoll, C. T., Likens, G. E., Holmes, R. T., Freuder, R. J. and Goodale, C. L.: 2002, 'Inorganic nitrogen losses from a forested ecosystem in response to physical, chemical, biotic, and climatic perturbations', *Ecosystems* **5**, 648–658.

Aber, J. D., McDowell, W. H., Nadelhoffer, K. J., Magill, A., Berntson, G., Kamakea, M., McNulty, S. G., Currie, W., Rustad, L. and Fernandez, I.: 1998, 'Nitrogen saturation in temperate forest ecosystems – hypotheses revisited', *Bioscience* **48**, 921–934.

Aber, J. D. and Driscoll, C. T.: 1997, 'Effects of land use, climate variation, and N deposition on N cycling and C storage in northern hardwood forests', *Global Biogeochem. Cycles* **11**, 639–648.

Aber, J. D., Ollinger, S. V. and Driscoll, C. T.: 1997, 'Modeling nitrogen saturation in forest ecosystems in response to land use and atmospheric deposition', *Ecol. Model.* **101**, 61–78.

Aber, J. D., Nadelhoffer, K. J., Steudler, P. and Melillo, J. M.: 1989, 'Nitrogen saturation in northern forest ecosystems', *Bioscience* **39**, 378–386.

Aber, J. D., Melillo, J. M. and Federer, C. A.: 1982, 'Predicting the effects of rotation length, harvest intensity, and fertilization on fiber yield from Northern hardwood forests in New England', *For. Sci.* **28**, 31–45.

Bohlen, P. J., Groffman, P. M., Driscoll, C. T., Fahey, T. J. and Siccama, T. G.: 2001, 'Plant-soil-microbial interactions in a northern hardwood forest', *Ecology* **82**, 965–978.

Bormann, F. H., Likens, G. E. and Melillo, J. M.: 1977, 'Nitrogen budget for an aggrading northern hardwood forest ecosystem', *Science* **196**, 981–983.

Bouraoui, F., Vachaud, G., Haverkamp, R. and Normand, B.: 1997, 'A distributed physical approach for surface-subsurface water transport modeling in agricultural watersheds', *J. Hydrol.* **203**, 79–92.

Campbell, J. L., Hornbeck, J. W., McDowell, W. H., Buso, D. C., Shanley, J. B. and Likens, G. E.: 2000, 'Dissolved organic nitrogen budgets for upland, forested ecosystems in New England', *Biogeochemistry* **49**, 123–142.

Campbell, G. S. and Norman, J. M.: 1998, *An Introduction to Environmental Biophysics,* 2nd edn., Springer-Verlag, New York, p. 304.

Christ, M. J., Peterjohn, W. T., Cumming, J. R. and Adams, M. B.: 2002, 'Nitrification potentials and landscape, soil and vegetation characteristics in two Central Appalachian watersheds differing in NO_3^- export', *For. Ecol. Manag.* **159**, 145–158.

Currie, W. S. and Nadelhoffer, K. J.: 1999, 'Dynamic redistribution of isotopically labeled cohorts of nitrogen inputs in two temperate forests', *Ecosystems* **2**, 4–18.

Dai, K. H., Johnson, C. E. and Driscoll, C. T.: 2001, 'Organic matter chemistry and dynamics in clear-cut and unmanaged hardwood forest ecosystems', *Biogeochemistry* **54**, 51–83.

Dail, D. B., Davidson, E. A. and Chorover, J.: 2001, 'Rapid abiotic transformation of nitrate in an acid forest soil', *Biogeochemistry* **54**, 131–146.

Driscoll, C. T., Lawrence, G. B., Bulger, A. J., Butler, T. J., Cronan, C. S., Eagar, C., Lambert, K. F., Likens, G. E., Stoddard, J. L. and Weathers, K. C.: 2001, 'Acidic deposition in the northeastern United States: Sources and inputs, ecosystem effects, and management strategies', *Bioscience* **51**, 180–198.

Eshleman, K. N., Morgan, R. P., Webb, J. R., Deviney, F. A. and Galloway, J. N.: 1998, 'Temporal patterns of nitrogen leakage from mid-Appalachian forested watersheds: Role of insect defoliation', *Water Resour. Res.* **34**, 2005–2016.

Fahey, T. J., Battles, J. J. and Wilson, G. F.: 1998, 'Responses of early successional northern hardwood forests to changes in nutrient availability', *Ecol. Monogr.* **68**, 183–212.

Fahey, T. J., Hughes, J. W., Pu, M. and Arthur, M. A.: 1988, 'Root decomposition and nutrient flux following whole-tree harvest of northern hardwood forest', *Forest Sci.* **34**, 744–768.

Federer, C. A.: 1995, 'BROOK90: A simulation model for evaporation, soil water, and streamflow', *General Technical Report NE-141*, USDA Forest Service, Durham, NH.

Fisk, M. C., Zak, D. R. and Crow, T. R.: 2002, 'Nitrogen storage and cycling in old- and second-growth northern hardwood forests', *Ecology* **83**, 73–87.

Fisk, M. C. and Fahey, T. J.: 2001, 'Microbial biomass and nitrogen cycling responses to fertilization and litter removal in young northern hardwood forests', *Biogeochemistry* **53**, 201–223.

Fitzhugh, R. D., Likens, G. E., Driscoll, C. T., Mitchell, M. J., Groffman, P. M., Fahey, T. J. and Hardy, J. P.: 2003, 'Role of soil freezing events in interannual patterns of stream chemistry at the Hubbard Brook Experimental Forest, New Hampshire', *Environ. Sci. Technol.* **37**, 1575–1580.

Fitzhugh, R. D., Driscoll, C. T., Groffman, P. M., Tierney, G. L., Fahey, T. J. and Hardy, J. P.: 2001, 'Effects of soil freezing disturbance on soil solution nitrogen, phosphorus, and carbon chemistry in a northern hardwood ecosystem', *Biogeochemistry* **56**, 215–238.

Gabrielle, B. and Kengni, L.: 1996, 'Analysis and field-evaluation of the CERES models' soil components: Nitrogen transfer and transformations', *Soil Sci. Soc. Am. J.* **60**, 142–149.

Gbondo-Tugbawa, S. S. and Driscoll, C. T.: 2002, 'Evaluation of the effects of future controls on sulfur dioxide and nitrogen oxide emissions on the acid-base status of a northern forest ecosystem', *Atmos. Environ.* **36**, 1631–1643.

Gbondo-Tugbawa, S. S., Driscoll, C. T., Aber, J. D. and Likens, G. E.: 2001, 'Evaluation of an integrated biogeochemical model (PnET-BGC) at a northern hardwood forest ecosystem', *Water Resour. Res.* **37**, 1057–1070.

Godde, M., David, M. B., Christ, M. J., Kaupenjohann, M. and Vance, G. F.: 1996, 'Carbon mobilization from the forest floor under red spruce in the northeastern U.S.A.', *Soil Biol. Biochem.* **28**, 1181–1189.

Goodale, C. L. and Aber, J. D.: 2001, 'The long-term effects of land-use history on nitrogen cycling in northern hardwood forests', *Ecol. Appl.* **11**, 253–267.

Goodale, C. L., Aber, J. D. and McDowell, W. H.: 2000, 'Long-term effects of disturbance on organic and inorganic nitrogen export in the White Mountains, New Hampshire', *Ecosystems* **3**, 433–450.

Gray, D. M. and Prowse, T. D.: 1993, 'Snow and floating ice', in D. R. Maidment (ed.), *Handbook of Hydrology*, McGraw-Hill, New York, pp. 7.1–7.58.

Groffman, P. M., Driscoll, C. T., Fahey, T. J., Hardy, J. P., Fitzhugh, R. D. and Tierney, G. L.: 2001, 'Effects of mild winter freezing on soil nitrogen and carbon dynamics in a northern hardwood forest', *Biogeochemistry* **56**, 191–213.

Hecky, R. E. and Kilham, P.: 1988, 'Nutrient limitation of phytoplankton in fresh-water and marine environments—A review of recent evidence on the effects of enrichment', *Limnol. Oceanogr.* **33**, 796–822.

Henriksen, A., Lien, L., Traaen, T. S., Sevalrud, I. S. and Brakke, D. F.: 1988, 'Lake acidification in Norway: Present and predicted chemical status', *Ambio* **17**, 259–266.

Hong, B.: 2004, 'Controls on the temporal and spatial patterns of streamflow nitrate flux at Hubbard Brook Watershed Six, New Hampshire, U.S.A.', Ph.D. Thesis, Cornell University, Ithaca, New York, U.S.A., p. 306.

Huntington, T. G. and Ryan, D. F.: 1990, 'Whole-tree-harvesting effects on soil-nitrogen and carbon', *For. Ecol. Manag.* **31**, 193–204.

Johnson, D. W.: 1992, 'Nitrogen retention in forest soils', *J. Environ. Qual.* **21**, 1–12.

Johnson, C. E., Johnson, A. H., Huntington, T. G. and Siccama, T. G.: 1991, 'Whole-tree clear-cutting effects on soil horizons and organic matter pools', *Soil Sci. Soc. Am. J.* **55**, 497–502.

Johnsson, H., Bergstrom, L., Jansson, P. E. and Paustian, K.: 1987, 'Simulated nitrogen dynamics and losses in a layered agricultural soil', *Agr. Ecosyst. Environ.* **18**, 333–356.

Kortelainen, P., Saukkonen, S. and Mattsson, T.: 1997, 'Leaching of nitrogen from forested catchments in Finland', *Global Biogeochem. Cycles* **11**, 627–638.

Likens, G. E., Driscoll, C. T., Buso, D. C., Siccama, T. G., Johnson, C. E., Lovett, G. M., Fahey, T. J., Reiners, W. A., Ryan, D. F., Martin, C. W. and Bailey, S. W.: 1998, 'The biogeochemistry of calcium at Hubbard Brook', *Biogeochemistry* **41**, 89–173.

Likens, G. E. and Bormann, F. H.: 1995, *Biogeochemistry of a Forested Ecosystem*, 2nd edn., Springer-Verlag, New York, p. 159.

Loehr, R. C., Prakasam, T. B. S., Srinath, E. G. and Joo, Y. D.: 1973, 'Development and demonstration of nutrient removal from animal wastes', *EPA Series Report R2-73-095*, USEPA, Washington, DC.

Lovett, G. M., Christenson, L. M., Groffman, P. M., Jones, C. G., Hart, J. E. and Mitchell, M. J.: 2002, 'Insect defoliation and nitrogen cycling in forests', *Bioscience* **52**, 335–341.

Lovett, G. M., Weathers, K. C. and Sobczak, W. V.: 2000, 'Nitrogen saturation and retention in forested watersheds of the Catskill Mountains, New York', *Ecol. Appl.* **10**, 73–84.

Lovett, G. M., Hart, J. E., Christenson, L. M. and Jones, C. G.: 1998, 'Caterpillar guts and ammonia volatilization: Retention of nitrogen by gypsy moth larvae consuming oak foliage', *Oecologia* **117**, 513–516.

Mayer, B., Boyer, E. W., Goodale, C. L., Jaworski, N. A., Van Breemen, N., Howarth, R. W., Seitzinger, S., Billen, G., Lajtha, K., Nadelhoffer, K., Van Dam, D., Hetling, L. J., Nosal, M. and Paustian, K.: 2002, 'Sources of nitrate in rivers draining sixteen watersheds in the northeastern U. S.: Isotopic constraints', *Biogeochemistry* **57**, 171–197.

Mitchell, M. J., Driscoll, C. T., Kahl, J. S., Likens, G. E., Murdoch, P. S. and Pardo, L. H.: 1996, 'Climatic control of nitrate loss from forested watersheds in the northeast United States', *Environ. Sci. Technol.* **30**, 2609–2612.

Murdoch, P. S., Baron, J. S. and Miller, T. L.: 2000, 'Potential effects of climate change on surface-water quality in North America', *J. Am. Water Resour. Assoc.* **36**, 347–366.

Murdoch, P. S., Burns, D. A. and Lawrence, G. B.: 1998, 'Relation of climate change to the acidification of surface waters by nitrogen deposition', *Environ. Sci. Technol.* **32**, 1642–1647.

Murdoch, P. S. and Stoddard, J. L.: 1992, 'The role of nitrate in the acidification of streams in the Catskill Mountains of New York', *Water Resour. Res.* **28**, 2707–2720.

Nadelhoffer, K. J., Downs, M. R., Fry, B., Magill, A. and Aber, J. D.: 1999, 'Controls on N retention and exports in a forested watershed', *Environ. Monit. Assess.* **55**, 187–210.

Ollinger, S. V., Smith, M. L., Martin, M. E., Hallett, R. A., Goodale, C. L. and Aber, J. D.: 2002, 'Regional variation in foliar chemistry and N cycling among forests of diverse history and composition', *Ecology* **83**, 339–355.

Parton, W. J., Scurlock, J. M. O., Ojima, D. S., Gilmanov, T. G., Scholes, R. J., Schimel, D. S., Kirchner, T., Menaut, J. C., Seastedt, T., Moya, E. G., Kamnalrut, A. and Kinyamario, J. I.: 1993, 'Observations and modeling of biomass and soil organic matter dynamics for the grassland biome worldwide', *Global Biogeochem. Cycles* **7**, 785–809.

Parton, W. J., Anderson, D. W., Cole, C. V. and Stewart, J. W. B.: 1983, 'Simulation of soil organic matter formations and mineralization in semiarid agroecosystems', in R. Lowrance, R. Todd, L. Asmussen and R. Leonard (eds.), *Nutrient Cycling in Agricultural Ecosystems*, University of Georgia Press, Athens, GA, pp. 533–550.

Perakis, S. S. and Hedin, L. O.: 2002, 'Nitrogen loss from unpolluted South American forests mainly via dissolved organic compounds', *Nature* **415**, 416–419.

Rawls, W. J., Ahuja, L. R., Brakensiek, D. L. and Shirmohammadi, A.: 1993, 'Infiltration and soil water movement', in D. R. Maidment (ed.), *Handbook of Hydrology*, McGraw-Hill, New York, pp. 5.1–5.51.

Robertson, G. P.: 1982, 'Nitrification in forested ecosystems', *Philos. Trans. R. Soc. B* **296**, 445–457.

Robertson, G. P. and Vitousek, P. M.: 1981, 'Nitrification potentials in primary and secondary succession', *Ecology* **62**, 376–386.

Ross, D. J. and Tate, K. R.: 1993, 'Microbial C and N, and respiratory activity, in litter and soil of a southern beech (*Nothofagus*) forest: Distribution and properties', *Soil Biol. Biochem.* **25**, 477–483.

Rosswall, T.: 1982, 'Microbiological regulation of the biogeochemical nitrogen cycle', *Plant Soil* **67**, 15–34.

Rutter, A. J., Kershaw, K. A., Robins, P. C. and Morton, A. J.: 1971, 'A predictive model of rainfall interception in forests, 1. Derivation of the model from observations in a plantation of Corsican pine', *Agric. Meteorol.* **9**, 367–384.

Schmidt, E. L.: 1982, 'Nitrification in soil', in F. J. Stevenson (ed.), *Nitrogen in Agricultural Soils*, American Society of Agronomy, Madison, WI, pp. 253–288.

Shuttleworth, W. J.: 1993, 'Evaporation', in D. R. Maidment (ed.), *Handbook of Hydrology*, McGraw-Hill, New York, pp. 4.1–4.53.

Steenhuis, T. S. and Van Der Molen, W. H.: 1986, 'The Thornthwaite-Mather procedure as a simple engineering method to predict recharge', *J. Hydrol.* **84**, 221–229.

Tierney, G. L. and Fahey, T. J.: 2001, 'Evaluating minirhizotron estimates of fine root dynamics in a northern hardwood forest', *Plant Soil* **229**, 167–176.

Tierney, G. L., Fahey, T. J., Groffman, P. M., Hardy, J. P., Fitzhugh, R. D. and Driscoll, C. T.: 2001, 'Soil freezing alters fine root dynamics in a northern hardwood forest', *Biogeochemistry* **56**, 175–190.

Tietema, A., Beier, C., De Visser, P. H. B., Emmett, B. A., Gundersen, P., Kjonaas, O. J. and Koopmans, C. J.: 1997, 'Nitrate leaching in coniferous forest ecosystems: The European field-scale manipulation experiments NITREX (nitrogen saturation experiments) and EXMAN (experimental manipulation of forest ecosystems)', *Global Biogeochem. Cycles* **11**, 617–626.

Verchot, L. V., Holmes, Z., Mulon, L., Groffman, P. M. and Lovett, G. M.: 2001, 'Gross vs net rates of N mineralization and nitrification as indicators of functional differences between forest types', *Soil Biol. Biochem.* **33**, 1889–1901.

Vitousek, P. M., Matson, P. A. and Van Cleve, K.: 1989, 'Nitrogen availability and nitrification during succession: Primary, secondary, and old-field series', *Plant Soil* **115**, 229–239.

Vitousek, P. M., Gosz, J. R., Grier, C. C., Melillo, J. M. and Reiners, W. A.: 1982, 'A comparative analysis of potential nitrification and nitrate mobility in forest ecosystems', *Ecol. Monogr.* **52**, 155–177.

Vitousek, P. M. and Melillo, J. M.: 1979, 'Nitrate losses from disturbed forests: Patterns and mechanisms', *For. Sci.* **25**, 605–619.

Whittaker, R. J., Likens, G. E., Bormann, F. H., Eaton, J. S. and Siccama, T. G.: 1979, 'The Hubbard Brook ecosystem study: Forest nutrient cycling and element behavior', *Ecology* **60**, 203–220.

Williard, K. W. J., De Walle, D. R., Edwards, P. J. and Schnabel, R. R.: 1997, 'Indicators of nitrate export from forested watersheds of the mid-Appalachians, United States of America', *Global Biogeochem. Cycles* **11**, 649–656.

Woodbury, P. B., Beloin, R. M., Swaney, D. P., Gollands, B. E. and Weinstein, D. A.: 2002, 'Using the ECLPSS software environment to build a spatially explicit component-based model of ozone effects on forest ecosystems', *Ecol. Model.* **150**, 211–238.

Zollweg, J. A.: 1994, 'Effective use of geographic information systems for rainfall-runoff modeling', Ph.D. Thesis, Cornell University, Ithaca, New York, U.S.A., p. 172.